Original Research Article

Electrooxidation of iohexol in its commercial formulation omnipaque on boron doped diamond electrode

ABSTRACT

This study investigated the electrochemical behavior of iohexol in its commercial formulation omnipaque on a boron-doped diamond electrode using cyclic voltammetry and chronoamperometry. The dependence of the anodic peak current density vs. iohexol concentration is linear and can be applied to the determination of the substrate concentration in environmental samples and pharmaceuticals. The iohexol electrooxidation on boron-doped diamond electrode is diffusion-controlled process and proceed via two ways: a direct electron transfers at the surface of boron-doped diamond electrode and an indirect oxidation mediated by *in situ* oxidative species. The iohexol electrooxidation in pH range from 2 to 6 includes exchange of 4 electrons and 1 proton, at pH superior to 6 it includes an exchanged of 2 electrons and 1 proton. The values of activation energy, anodic transfer coefficient, heterogenous rate constant, diffusion coefficient and the catalytic rate constant were 14.164 kJ mol^{-1}, 0.428, 1.06×10^{3} s^{-1}, 4.47×10^{-6} cm^{2} s^{-1} and 3.61×10^{2} M^{-1} s^{-1} respectively. It appears from those results that, on our electrode, for the high potential scan rates, few actives sites mainly those located at the electrode surface are involved in the iohexol oxidation process. As the potential scan rate decreases, more actives sites are involved in the process.

Keywords: Iohexol, Electrochemical oxidation, Cyclic voltammetry, boron-doped diamond

1. INTRODUCTION

Iodinated X-ray contrast media (ICM), mainly constituted by 2,4,6-triiodinated benzoic acid derivatives, are pharmaceutical products used in medicine in large quantities to allow better visualization of blood vessels and organs during diagnosis [1]. After injection, ICMs are almost completely ejected from the human body within 24h [2]. Thus, ICMs are detected in water samples at concentrations ranging from ng L^{-1} to µg L^{-1} [1]. Among ICMs, iohexol is commonly detected at high concentrations in water samples due to its incomplete degradation by conventional wastewater treatment processes [3, 4]. We can find in literature some studies about iohexol (IOX) degradation [2, 3, 5] and more recently a paper was released about IOX determination by differential pulse voltammetry on a micro boron doped diamond (BDD) electrode [6]. but less works has been performed on cyclic voltammetry (CV) and chronoamperometry. CV is a powerful and simple electrochemical technique. It is commonly used to understand the oxidation and reduction mechanisms of molecular species

[7]. On the other hand, it allows the study of chemical reactions [8, 9]. CV is also very useful for studying chemical reactions initiated by electron transfer. Indeed, this technique allows the qualitative and quantitative study of a processes taking place at the electrode/electrolyte interface [10-12]. Chronoamperometry is an electrochemical technique used generally to determine kinetic parameters such as the diffusion coefficient and the catalytic rate constant [13,14]. For its application, this electrochemical technique requires the use of electrodes with specific properties. In fact, the electrooxidation of organic compounds takes place in two ways: direct transfer of electrons to the electrode and/or oxidation mediated by oxidizing species formed from water or other species that discharge on the electrode surface [15]. Boron-doped diamond (BDD) electrode, due to its good properties, has been considered as an electrode of choice for the removal of environmental contaminants [15, 16]. The objective of this work is to study the electrochemical behavior of IOX by CV and chronoamperometry on BDD electrode. The effect of scan rate, substrate concentration, temperature and pH on the electrooxidation of IOX will be examined.

2. EXPERIMENTAL

2.1. Measurement methods

Cyclic voltammetry (CV) and chronoamperometry was used in electrochemical measurements carried out in an Autolab Potentiostat of ECHOCHEMIE (PGSTAT 20) ordered by a computer (Software GPES) allowing a data-processing acquisition of the data. A three-electrode electrochemical cell composed of a BDD as the working electrode, the geometric surface of contact between the BDD and the electrolyte is 1 cm^2. A saturated calomel electrode (SCE) as a reference electrode put in a capillary luggin placed at approximately 2 mm of the working electrode in order to overcome the potential ohmic drop. A platinum wire was used as a counter electrode (CE). A thermoregulator MGW LAUDA connected to the electrochemical cell was used for the variation of the temperature. pH of electrolytes was measured using a probe pH-meter HI2211 with glass electrode.

2.2. Chemicals

Omnipaque (iohexol) was purchased from a pharmacy in Abidjan. Electrolytes used in this study were prepared with sulphuric acid (Fluka). The pH of the electrolyte was adjusted using sodium hydroxide (Prolabo). The solid products and reagents are stored at the ambient temperature and safe from the light. Solutions were prepared using distilled water. All the experiments were made at ambient temperature of 25 °C.

3. RESULTS AND DISCUSSION

3.1. Influence of varying IOX concentration

The voltammetric curves presented in Figure 1 show the behaviour of the BDD electrode in the presence and absence of IOX in the H_2SO_4 (0.1M) electrolyte support. In the absence of IOX, we observe a normal BDD curve with oxygen evolution reaction at 2.27 V vs. SCE [17, 18]. With the addition of IOX, a rapid increase in current is observed from 1.86 vs. SCE followed by an oxidation peak at 2.12 V vs. SCE. This peak is characteristic of IOX oxidation. In the backward potential scan of the voltammograms, no characteristic peak of IOX reduction was observed. These observations indicate the irreversibility of the electrochemical process. The variation in concentration is a kinetic parameter frequently used in electrooxidation of organic compounds. The study of the variation of the IOX concentration on the DDB electrode was carried out for a range of IOX concentration from

1.2 to 3.2 mM. Voltammetric curves were recorded at a scan rate of 50 mV s^{-1} in a potential domain from -1.5 V vs. SCE to 3 V vs. SCE in H_2SO_4 (0.1 M) media.

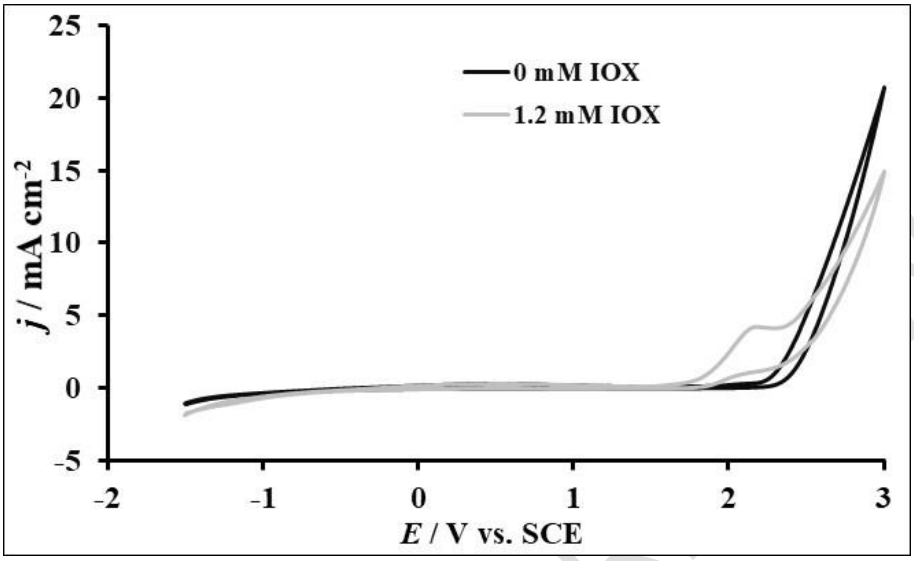

Figure 1. Cyclic voltammograms of BDD in 0.1 M H_2SO_4 in presence and absence of IOX at 50 mV/s.

Figure 2A shows the results obtained. With the addition of IOX, the oxygen evolution reaction becomes faster. An increase in the peak oxidation peak current densities is noted with the increase of IOX concentration. This shows that the electrochemical process during the oxidation of IOX on BDD in H_2SO_4 media could be controlled by diffusion [19]. For IOX concentrations ranging from 1.2 to 2 mM, the oxidation peaks of IOX appear in the stability range of the electrolytic media (0.1 M H_2SO_4), the IOX oxidation is direct and results from an electronic transfer at the interface electrolyte / BDD. For IOX concentrations superior than 2 mM, oxidation peaks appear beyond the electroactivity domain of BDD.

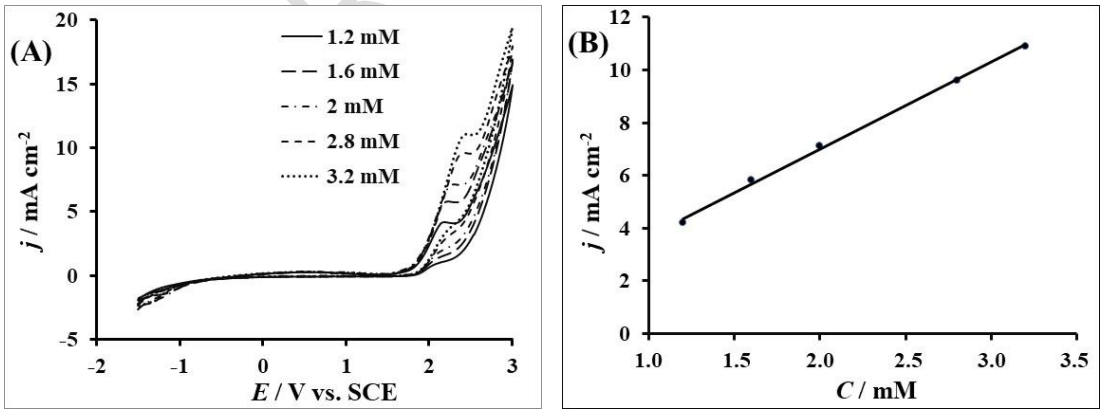

Figure 2. (A) Cyclic voltammetry curves recorded on the BDD in H_2SO_4 (0.1M) in the presence of different IOX concentrations at 50 mV s^{-1}; (B) plot of current density of the IOX oxidation peak versus IOX concentrations.

Thus, the oxidation of IOX could be indirect and facilitated by the participation of oxidative species such as weakly adsorbed hydroxyl radicals on BDD surface, resulting from the

electrochemical decomposition of water. These results indicate that the IOX degradation on this electrode can be done either by a catalytic oxidation mechanism involving direct oxidation of IOX on electrode surface, i.e. direct transfer of electron to the surface of the electrode, or by indirect oxidation involving the adsorbed hydroxyl radicals or other oxidative species produced *in-situ*.
The evolution of the current density oxidation peak as a function of the concentration was studied. The result obtained is presented in the box in Figure 2B. This figure shows that the current density of the oxidation peak increases linearly with the concentration (determination coefficient R^2 = 0.998) by describing an affine line (equation 1).

$$j_P = 3.2969\ C + 0.4091 \quad (1)$$

With j_P: the current density (mA cm^{-2}) and C: the IOX concentration (mM).

The determination coefficient (R^2) was determined using Microsoft Excel. The value of the determination coefficient R^2 = 0.998 close to 1 shows the good linearity of the increase of IOX oxidation peak current density j_P with the IOX concentration. This linearity also shows that BDD can be used for a quantitative determination of IOX [20].

3.2 Effect of the number of potential scanning cycles

During voltammetric measurements, it is important to ensure that during the electrooxidation of organic compounds, the electrode used does not become covered with a polymeric or insulating film on its surface. For this reason, several potential scan cycles were performed on the BDD electrode in H_2SO_4 media containing 3.2 mM IOX. Figure 3A shows the voltamograms obtained by varying the number of cycles on the BDD in a potential range from -1.5 V vs. SCE to 3 V vs. SCE under a potential scan rate of 50 mV s^{-1}. A decrease in the oxidation peak from cycle 1 to cycle 4, and then a superposition of the voltammetric curves from cycle 4 to cycle 16 are observed. These different observations show that there is no formation of inhibitory polymeric film on the surface of BDD during the electrooxidation of OMP in H_2SO_4 media.

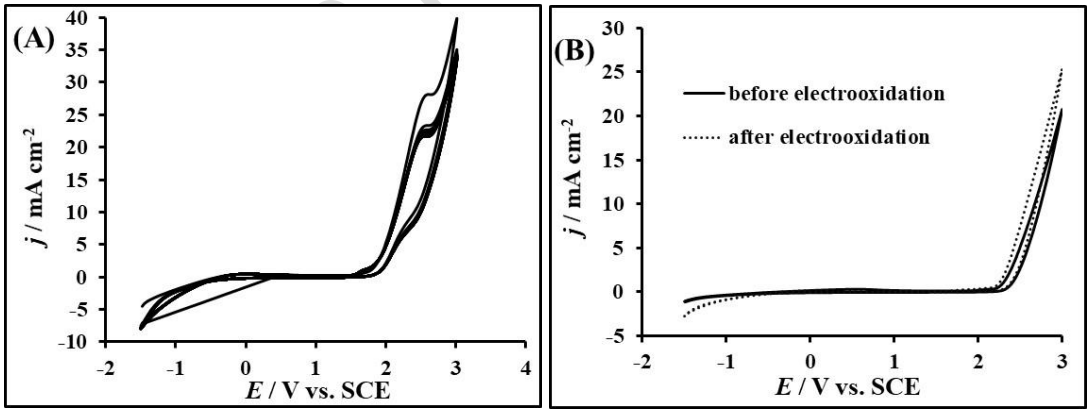

Figure 3: (A) Cyclic voltammogram of BDD in 0.1 M H_2SO_4 for 23 successive Cycles in scans performed; (B) Cyclic voltammogram of BDD in 0.1 M H_2SO_4 before and after electrooxidation.

After these 23 cycles, the electrochemical characterization of BDD in H_2SO_4 (0.1 M) media was resumed and compared to the curve obtained in H_2SO_4 media before IOX oxidation. The voltammetric curves obtained are shown in Figure 3B. After electrochemical oxidation, the voltamogram obtained is characterized by an absence of an oxidation peak, an

electroactivity domain identical to that obtained before electrooxidation and an increase in current density of 0.005 A. The quasi-superposition of the obtained curves indicates that the BDD electrode would be suitable for a probable degradation of IOX in aqueous media.

3.3. Influence of temperature variation

The effect of temperature on the oxidation of IOX was studied in a sulfuric acid solution (0.1 M) containing 3.2 mM of IOX at 50 mV / s. The results obtained are shown in Figure 4A. A decrease in the oxygen evolution potential is observed from 1.56 V vs. SCE at 25 °C to 1.45 V vs. SCE at 82 °C. Thus, it appears that the IOX oxidation becomes faster with increasing temperature. These results could be explained by *in-situ* production of hydroxyl radicals by electrochemical decomposition of water and / or iodine during IOX oxidation.

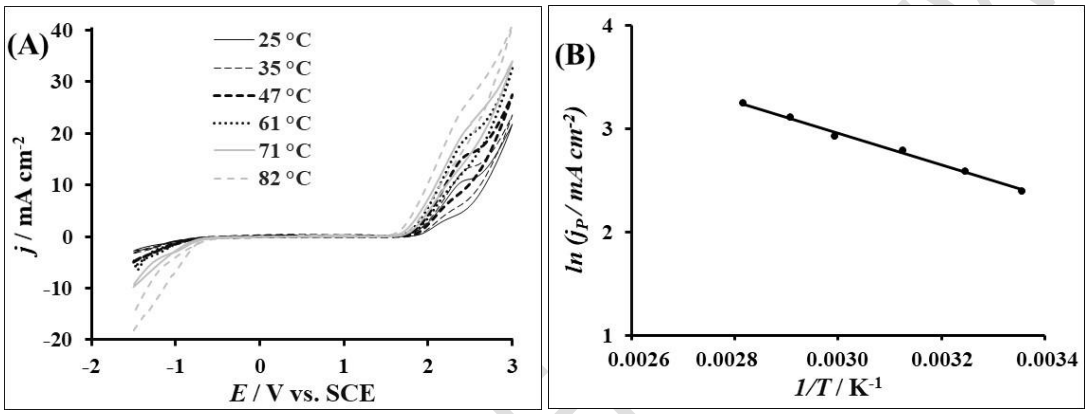

Figure 4. A) Cyclic voltammetry curves recorded on BDD electrode at several temperatures in 0.1 M H_2SO_4 containing 3,2 mM IOX under the potential scan rate: 50 mV s^{-1}, (B) plot of ln Ip = f (1/T)

Figure 4A also shows an increase in the oxidation current density with temperature. On the other hand, the plot of the natural logarithm as a function of the inverse of the temperature (Figure 4B) gives a line with a determination coefficient 0.996 and the following equation:

$$\ln j_P = -1704.5 \frac{1}{T} + 1.137 \qquad (2)$$

With j_P : peak current density (A cm^{-2}) and T: temperature (K). The activation energy (Ea) of the reaction equal to 14.164 kJ mol^{-1} was estimated using the slopes of equations 2 and 3 [21].

$$E_a = -R \left(\frac{\partial \ln j_P}{\partial (1/T)}\right) \qquad (3)$$

This value of the activation energy lower than 40 kJ mol^{-1} indicates that the IOX oxidation is controlled by diffusion [22, 23].

3.4. Influence of the scan rate

The potential scan rate provides a lot of information about the processes occurring at the electrode / electrolyte interface. The voltammetric responses recorded on the BDD in the presence of IOX (3.2 mM) at potential scan rates ranging from 20 mV s^{-1} to 100 mV s^{-1} in H_2SO_4 are shown in Figure 5. This figure shows an increase of the current density of the oxidation peak (j_P) with increasing potential scan rate.

Reversibility and kinetic regime (adsorption or diffusion) can be studied by analyzing the dependencies of the oxidation peak current density (j_P) as a function of the square root of the scan rate ($v^{1/2}$) and the logarithm of the peak current density (log j_P) as a function of the logarithm of the scan rate (log v) [24, 25].
For the first approach, the curve j_P versus $v^{1/2}$ was plotted (Figure 6A). The curve obtained is a straight line with a determination coefficient $R^2 = 0.998$. This shows the very good linearity between the oxidation peak current density (j_P) and the square root of the scan rate in ($v^{1/2}$). However, this dependence does not intercept the axis origin. According to the literature, the electrochemical process could be preceded or followed by a homogeneous chemical reaction and controlled by adsorption [26, 27].
The second approach is summarized by plotting the curve log j_P vs. log v. The resulting curve shown in Figure 6B is a straight line described by the equation (4):

$$\log j_P = 0.304 \log v - 1.154 \quad (4)$$

With j_P : peak current density (A cm^{-2}) and v: scan rate (V s^{-1}).

The slope of the log j_P vs. log v has a value of 0.304 close to 0.5. This confirms a process at the electrode limited by diffusion and preceded by a chemical reaction [27-29].
According to these two approaches, the electrochemical process during the electrooxidation of IOX on BDD in H_2SO_4 media is limited by the diffusion of the substrate on the BDD and preceded by a chemical reaction.

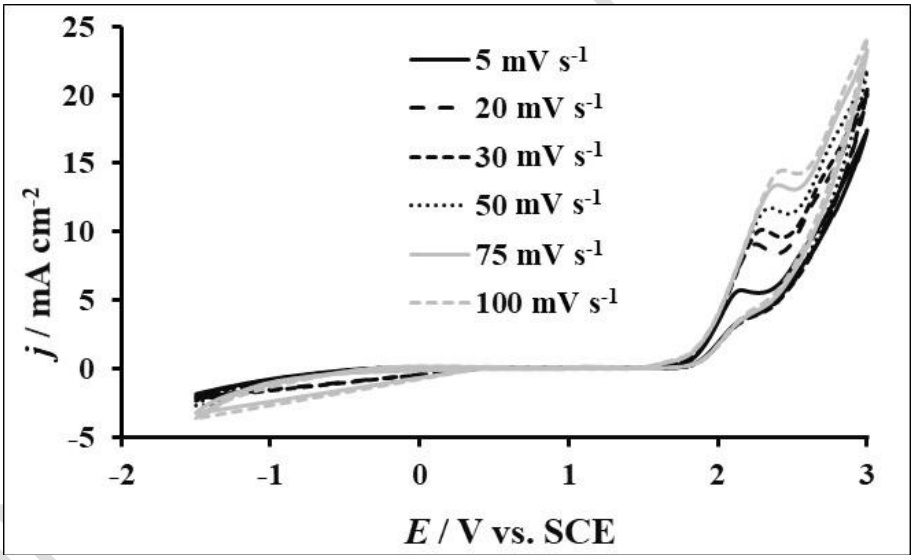

Figure 5: Cyclic voltammetry curves recorded on BDD electrodes in 3,2 mM IOX containing in 0.1 M H_2SO_4 at several potential scan rates (5-100 mV s^{-1}).

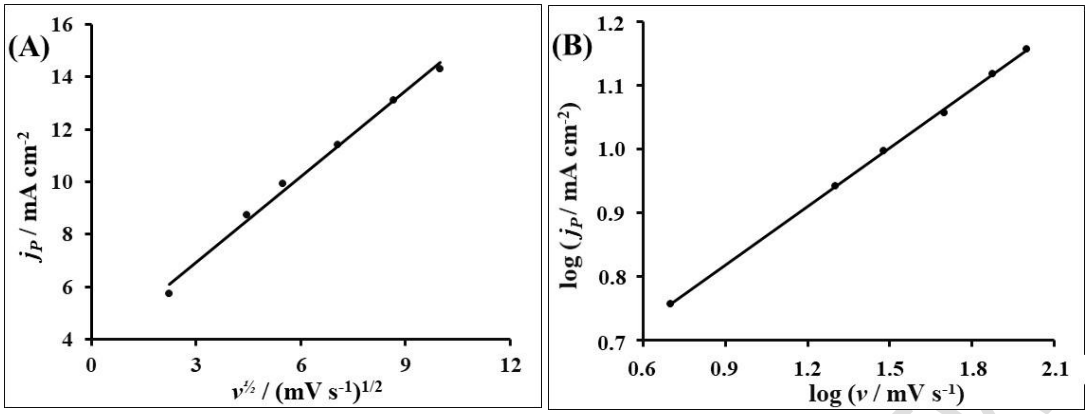

Figure 6: (A) Evolution of the peak of current density against the square root of the potential scan rates j_P vs. $v^{1/2}$. (B); Plot of log j_P vs. log *v*.

In Figure 6A, we record the curve Ep vs. *v* of the oxidation peak potential as a function of the potential scan rate. The potential of the oxidation peak increases and shift with the scan rate. The heterogeneous electron transfer during the electrooxidation of IOX at BDD in the used electrolyte support is therefore irreversible [27] i.e. a slow electron exchange of the redox species with the BDD electrode [30].
Figure 6B shows the curve of the potential of the oxidation peak (Ep) as a function of the logarithm of the scan rate (log *v*). The dependence of Ep vs. log *v* is linear with a determination coefficient 0.985 and described by the equation 5:

$$Ep = 0.138 \log v + 2.531 \quad (5)$$

With E_P: peak potential (V) and *v*: scan rate (V s^{-1}).
The Laviron expression corresponding to an irreversible electrode process [31, 32] is described by the following equation:

$$E_P = \left(\frac{2.303\ RT}{\alpha\ n\ F}\right) \log v + E^0 + \left(\frac{2.303\ RT}{\alpha\ n\ F}\right) \log \left(\frac{RTk^0}{\alpha\ nF}\right) \quad (6)$$

Where Ep is the peak potential in V, E^0 the formal potential in V, R is the universal gas constant (8.314 J K^{-1} mol^{-1}), T is the temperature in Kelvin (298 K), n is the number of electrons involved, k^0 is the standard heterogenous rate constant of the reaction (s^{-1}), F is Faraday's constant (96487 C mol^{-1}), α is the anode transfer coefficient and v is the potential scan rate (V s^{-1}).
Using the slope of equations (5) and (6), αn was calculated to be 0.428. For a totally irreversible electrode process, the electron transfer coefficient α is assumed to be 0.5 [33, 34]. Thus, the number of electrons involved was calculated to be 0.857 ≈ 1. The electrooxidation of IOX at BDD involved one electron transfer phenomenon.
The formal potential E^0 and the standard heterogeneous rate constant k^0 were estimated using respectively the intercept of the curves Ep vs.ν (Figure 7A) for ν = 0 and Ep vs. log v (Figure 7B). Values of E^0 and k^0 were 2.28 and 1.06 x 10^3 s $^{-1}$ respectively.

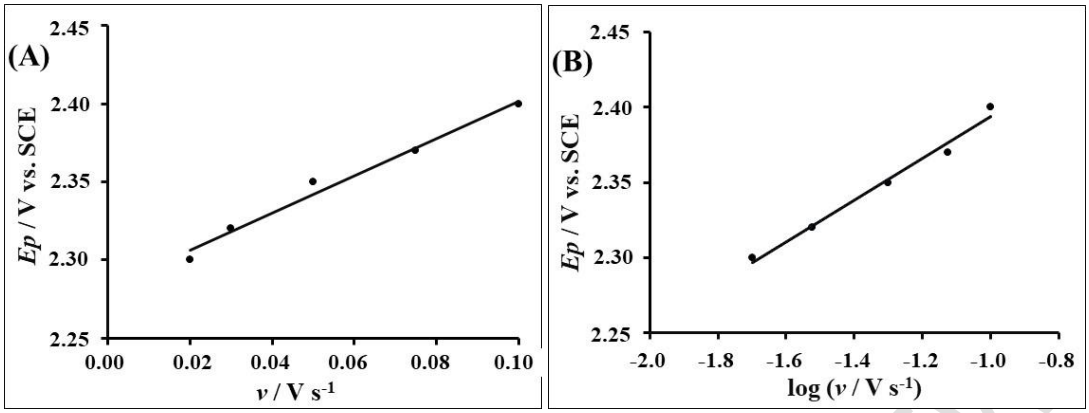

Figure 7: (A) Dependence of peak potential (Ep) on the potential scan rate (*v*); (B) Variation of the scan rate normalized current with scan rate.

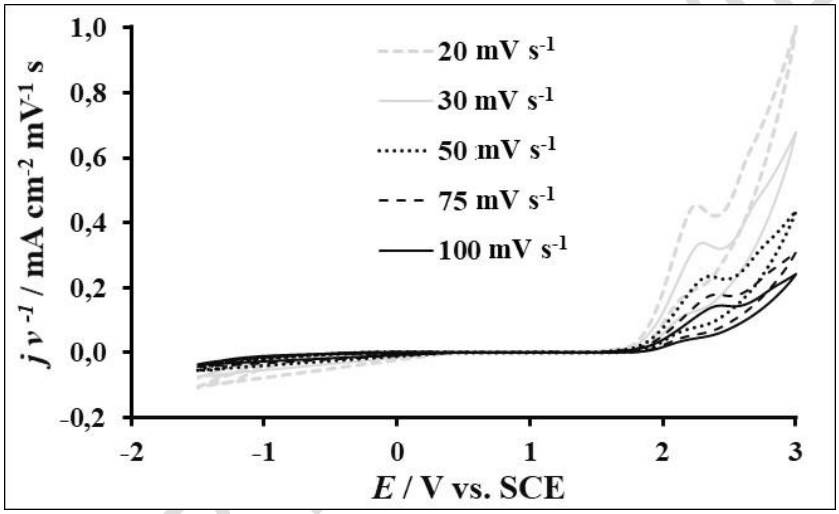

Figure 8: Normalized current density of the cyclic voltammetry measurement recorded on (A) BDD in 0.1 M H_2SO_4 containing 3,2 mM IOX with the potential scan rates (20-100 mV s^{-1}) versus applied potential

In Figure 8, normalized current density, obtained through the ratio of the current density over the potential scan rates, were plotted against the applied potential on the electrode. In this figure, as the potential scan rates increase, the capacitance decreases indicating that for the low potential scan rates, more electrode active sites intervene in the surface processes. It appears from those results that, on our electrode, for the high potential scan rates, few actives sites mainly those located at the electrode surface are involved in the IOX oxidation process. As the potential scan rate decreases, more actives sites, composed by those at the electrode surface and those in the pores are involved in the process.

3.5. Influence of pH

The influence of pH on IOX oxidation was studied. The results obtained for pH values ranging from 1.2 to 12.1 are shown in Figure 9. This figure shows a shift towards the positive potentials of IOX oxidation peak and a decrease in the current density of oxidation peak when the pH is acidic (from 2 to 6).

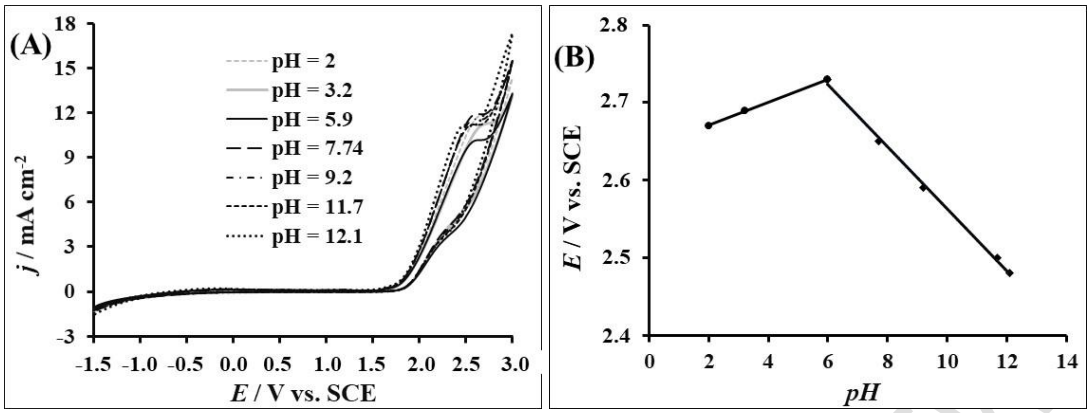

Figure 9: (A) Cyclic voltammograms recorded on BDD at different pH in H_2SO_4 (0.1 M) containing 3.2 mM of IOX at 50 mV s^{-1}; (B) Peak potential as a function of pH

For basic pH (7.7 to 12.1), the oxidation peak shifts to the left with increasing pH. This suggests different IOX oxidation mechanisms in acidic and basic environments. This reduction in the current density of the oxidation peak in an acidic media could reflect the intervention of H^+ protons in this electrochemical reaction. We also note that the oxidation peak becomes less marked, turning into an oxidation peak with increasing pH. According to Koffi and al. [35], this result can be explained by the effect of the very strong electrostatic repulsion between the surface of the BDD and the species in solution.
The linear relations of the segments of Ep vs. pH for acidic pH (equation 7) and for basic pH (equation 8) are described by the equations:

$E_P(V)$= 0.0149 pH + 2.641 (7)

$E_P(V)$ = -0.04 pH + 2.964 (8)

The m/n ratio represents the number of protons (m) and electrons (n) exchanged during the electrooxidation of IOX and was calculated using the following equation.

$$\frac{dEp}{dpH} = \frac{2.303mRT}{nF} \quad (9)$$

Thus, for pH values ranging from 2 to 6, the m/n ratio equals 0.25. This value reflects 1 proton and 4 electrons exchanged during the electrochemical oxidation process for acidic pH.
At pH values from 7.7 to 12.1, the calculated m/n ratio equals 0.67. There is therefore an exchange of two electrons and one proton during the electrochemical oxidation of IOX for basic pH.

3.6. Determination of the diffusion coefficient and the catalytic rate constant

For any chronoamperometric measurement, one of the most important factors is the potential to be imposed. In the case of the BDD electrode, it should be noted that the voltammetric study revealed the presence of an anodic oxidation peak for IOX. Thus, the measurements were performed at the potential of the IOX oxidation peak which also corresponds to the highest current density. Figure 10 the chronoamperometric curves obtained in the absence and presence of IOX in H_2SO_4 media (0.1 M). In the absence of IOX, a regular curve with two parts is observed. For a duration lower than 22 s, a fall of the current density which varies from 6 to 1.8 mA cm^{-2} is observed. This rapid decrease in

current density could be explained by a discharge of the electric double layer. For longer durations (t > 22 s), we observe a quasi-constant evolution of the current density at a current density j = 1.8 mA cm^{-2} which can be explained by a diffusion of the ions present in solution or that the diffusion is the kinetically determining mass transport mode.
We also note an increase in the stationary and faradic current densities in the absence and presence of IOX which evolve respectively from 6 to 20 mA cm^{-2} and from 1.8 to 4.5 mA cm^{-2}. The increase in current density could be explained by the consumption of the electroactive species (IOX) on the surface of the BDD.

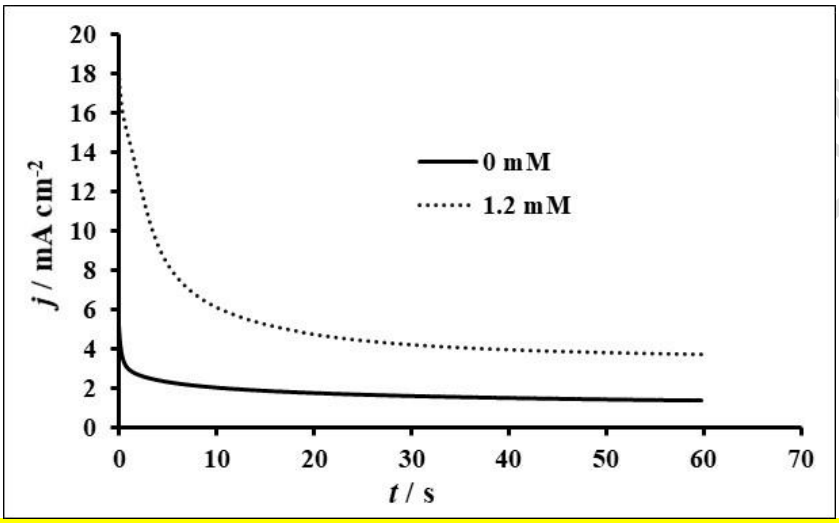

Figure 10: Chronoamperometric curves in 0.1 M H_2SO_4 (pH = 9), in the absence and presence of 1.2 mM OMP

Figure 11A shows the results from varying the concentration of IOX in H_2SO_4 media (0.1 M) at a fixed potential of 2.3 V vs. SCE. The stationary current density increases with increasing IOX concentration. From 2 mM IOX, the faradaic current decreases with IOX concentration and rapidly decreases by about 20 % of its initial value before 20 s. The plot of the stationary current density versus IOX concentration is shown in Figure 11B. The resulting j vs. C curve is a straight line described by the equation below:

$$j = 2.142.C + 0.995 \quad (10)$$

The value of the determination coefficient (R^2 = 0.995) indicates the linearity between current density and OMP concentration.

In Figure 12A, is presented the Cottrell j vs. $t^{-1/2}$ curve performed for 3.2 mM IOX. The curve obtained is a straight line where the current density decreases monotonically with ($t^{-1/2}$). Moreover, it should be noted that the observed linearity obeys the following Cottrell equation for a plane electrode and for an electrochemical reaction limited by mass transport [13]:

$$j = nFAC\left(\frac{D}{\pi t}\right)^{1/2} \quad (11)$$

Where j represents the current density, n the number of moles of electrons exchanged, F the Faraday constant, C the molar concentration of the solution, t the time during which the potential is applied, D the diffusion coefficient and A the surface area of the electrode.

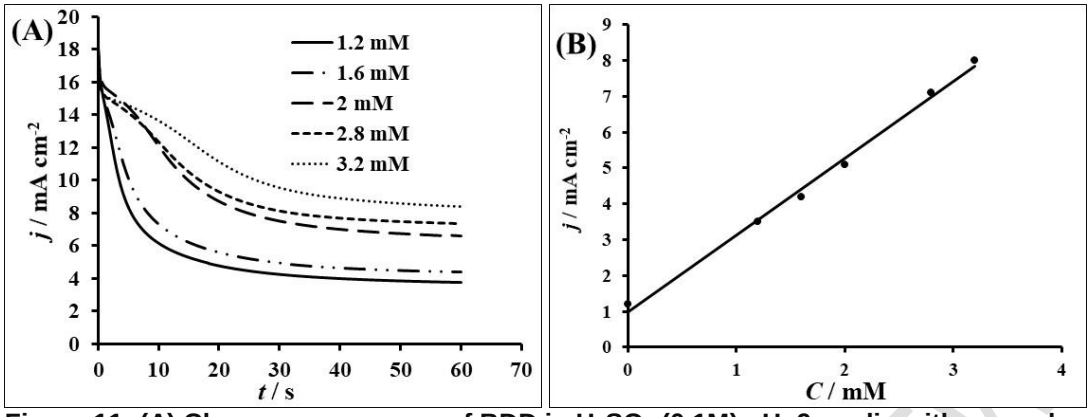

Figure 11: (A) Chronoamperogram of BDD in H_2SO_4 (0.1M) pH=9 media with several concentrations of IOX. Applied potential E = 2.4 V vs. SCE; (B) Current density versus IOX concentration curve.

According to the voltammetric study (effect of pH), for a pH = 9, the number n of electrons exchanged during the electrooxidation of OMP is equal to 2.
Thus, by equalizing the slopes of equation (11) and the equation of the j vs. $t^{-1/2}$ curve ($j = 0.737\ t^{-1/2} + 14.465$), the diffusion coefficient was estimated to be 4.47×10^{-6} $cm^2\ s^{-1}$.

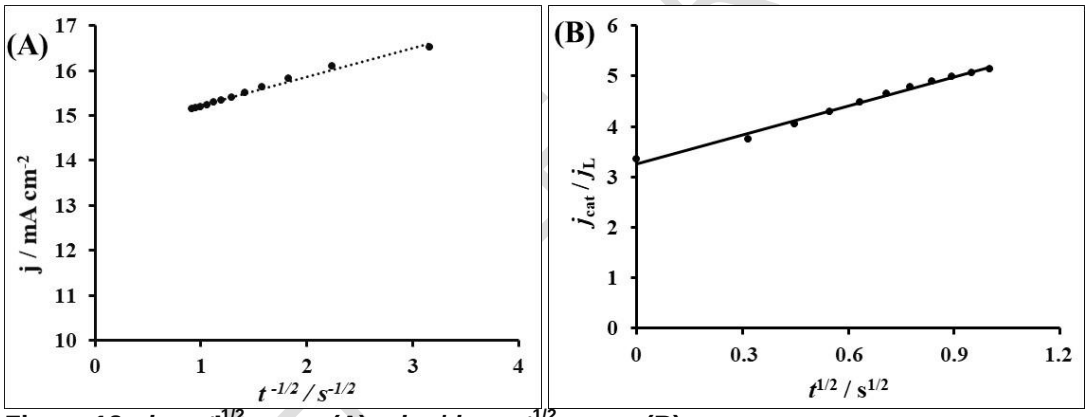

Figure 12 : j vs. $t^{-1/2}$ curve (A) ; j_{cat} / j_L vs. $t^{1/2}$ curve (B)

Chronoamperometry was also used to determine the value of the catalytic rate constant k_{cat}, at the electrode/electrolyte interface. For an intermediate time, when the rate of the electrocatalytic reaction dominates the oxidation current density, the catalytic current density j_{cat} can be defined by the following equation [14]:

$$\frac{j_{cat}}{j_L} = \pi^{1/2}(k_{cat} \times C_0 \times t)^{1/2} \qquad (12)$$

Where, j_{cat} and j_L represent the current densities in the presence and absence of IOX, respectively. k_{cat}, the catalytic rate constant ($M^{-1}\ s^{-1}$), C_0, the concentration of IOX (M) and t, the elapsed time (s).
The j_{cat} / j_L vs $t^{1/2}$ curve shown in Figure 12B is a straight line described by the equation:

$$j_{cat} / j_L = 1.907\ t^{1/2} + 3.263 \qquad (13)$$

The value of the catalytic rate constant k_{cat} was calculated from the slopes of equations (12) and (1 3). The value of k_{cat} obtained is 3.61×10^{-2} M^{-1} s^{-1}.

4. CONCLUSION

The electrooxidation of IOX has been studied on BDD in a sulfuric acid media. The electrooxidation of IOX is irreversible and proceeds by diffusion of IOX onto the BDD followed by a chemical reaction. The linearity of the dependence of the oxidation peak of the current density on the IOX concentration shows that BDD can be applied to the determination of IOX concentration in environmental and pharmaceutical samples. The electrooxidation of IOX in the pH range 2 to 6 involves an exchange of 4 electrons and 1 proton, at pH superior 6 it includes an exchange of 2 electrons and 1 proton. The values of the activation energy, anodic transfer coefficient and the standard heterogeneous rate constant are respectively, 14.164 kJ mol^{-1}, 0.428 and $1.06x10^{3}s^{-1}$. Chronoamperometry study allows to estimate the diffusion coefficient of IOX and the catalytic rate constant, respectively to 4.47×10^{-6} cm^2 s^{-1} and 3.61×10^{2} M^{-1} s^{-1}.

COMPETING INTERESTS DISCLAIMER:

Authors have declared that no competing interests exist. The products used for this research are commonly and predominantly use products in our area of research and country. There is absolutely no conflict of interest between the authors and producers of the products because we do not intend to use these products as an avenue for any litigation but for the advancement of knowledge. Also, the research was not funded by the producing company rather it was funded by personal efforts of the authors

REFERENCES

1. Wang X, Wang Z, Tang Y, Xiao D, Zhang D, Huang Y, Guo Y, Liu J. Oxidative degradation of iodinated X-ray contrast media (iomeprol and iohexol) with sulfate radical: An experimental and theoretical study. Chemical Engineering Journal. 2019; 368: 999–1012. https://doi.org/10.1016/j.cej.2019.02.194
2. Hu C-Y, HouY-Z, Yi-Li L, Deng Y-G, Hua S-J, Yi-Fan D, Chen C-W, Wu C-H. Investigation of iohexol degradation kinetics by using heat-activated persulfate. Chemical Engineering Journal. 2020; 379: 122403. http://dx.doi.org /10.1016/j.cej.2019.122403
3. Turkay O, Barisci S, Ulusoy E, Dimoglo A. Electrochemical Reduction of X-ray Contrast Iohexol at Mixed Metal Oxide Electrodes: Process Optimization and By-product Identification. Water Air Soil Pollut. 2018; 229: 170. https://doi.org/10.1007/s11270-018-3823-0
4. Wang Z, Lin Y-L, Xu B, Xia S-J, Zhang T-Y, Gao N-Y. Degradation of iohexol by UV/chlorine process and formation of iodinated trihalomethanes during post-chlorination. Chemical Engineering Journal. 2016; 283: 1090–1096. https://doi.org/10.1016/j.cej.2015.08.043
5. Tissot GB, Anglada A, Dimitriou-Christidis P, Rossi CL, Arey JS, Comninellis Ch. Kinetic experiments of electrochemical oxidation of iohexol on BDD electrodes for wastewater treatment. Electrochemistry Communications. 2012; 23: 48–51. https://doi:10.1016/j.elecom.2012.07.006
6. Koffi KS, Appia FTA, Kouadio KE, Kimou KJ, Koné S, Ouattara L. Cyclic and differential pulse voltammetry investigations of an iodine contrast product using microelectrode of BDD.

Mediterranean Journal of Chemistry. 2021; 11(3): 244-254.http://dx.doi.org/10.13171/mjc02109301594lassin%C3%A9
7. Gomaa EA, El-Dossoki FI, Zaky RR, Shabaan S, Attia FA. Cyclic Voltammetric studies of the interaction of cupric chloride with (Z)-4-oxo-4-((4-selenocyannatophenyl)amino) but-2-2nonic acid , (Chal) in KCl solutions using glassy carbon electrode. Egyptian Journal of Chemistry. 2021; 64(5): 2671 - 2678. DOI: 10.21608/EJCHEM.2021.44261.2903
8. Salem SE, Gomaa EA, El-Defraway MM, Mohamed NM. Studies on the Complexation of Succinic Hydrazide with Copper Chloride Salt. European Journal of Advanced Chemistry Research. 2021; 2 (1): 14-20. http://dx.doi.org/10.24018/ejchem.2021.2.1.40
9. Fathi M, Salem SE, Gomaa EA, Killa HM, Farouk A. Study of Electrochemical Redox Reaction of $CuSO_4$ Salt with Amoxicillin at Different Temperatures Using Glassy Carbon Electrode. Egyptian Journal of Chemistry. 2020; 63(12): 5239 – 5249. DOI: 10.21608/EJCHEM.2020.24886.2477
10. Arshad N, Zafran M, Ashraf Z, Perveen F. Synthesis, characterization of amide substituted dexibuprofen derivatives and their spectral, voltammetric and docking investigations for DNA binding interactions. Journal of Photochemistry and Photobiology B: Biology. 2017; 169: 134-147. https://doi.org/10.1016/j.jphotobiol.2017.02.021
11. Kouadio KE, Kambiré O, Koffi KS, Ouattara L. Electrochemical oxidation of paracetamol on boron-doped diamond electrode: analytical performance and paracetamol degradation. J. Electrochem. Sci. Eng. 2021; 11(2): 71-86. DOI: https://doi.org/10.5599/jese.932
12. Kambiré O, Pohan LAG, Sadia SP, Kouadio KE, Ouattara L. Voltammetric study of formic acid oxidation via active chlorine on IrO_2/Ti and RuO_2/Ti electrodes. Mediterranean Journal of Chemistry. 2020; 10(8): 799-808. DOI: http://dx.doi.org/10.13171/mjc10802010271525ko
13. Zare M, Sarhadi H. A novel vitamin B9 sensor based on modified screen-printed electrode J. Electrochem. Sci. Eng. 2021; 11(1): 1-9. http://dx.doi.org/10.5599/jese.878
14. Zhang R, Liu L, Li Y, Wang W, Li R. Electrooxidation Kinetics of Hydrazine on Y-type Zeoliteencapsulated Ni(II)(salen) Complex Supported on Graphite Modified Electrode. Int. J. Electrochem. Sci. 2015; 10: 2355 - 2369
15. Quand-Meme GC, Auguste AFT, Hélène LEM, Mohamed B, Placide SS, Sanogo I, Ouattara L. Electrooxidation of ceftriaxone in its commercial formulation on boron doped diamond anode. J. Adv. Electrochem. 2016; 2(2): 85–88.
https://doi.org/10.4236/ajac.2019.1011039
16. He Y, Lin H, Guo Z, Zhang W, Li H, Huang W. Recent developments and advances in boron-doped diamond electrodes for electrochemical oxidation of organic pollutants. Separation and Purification Technology. 2019; 212: 802-821.
https://doi.org/10.1016/j.seppur.2018.11.056
17. Kambiré O, Alloko KSP, Pohan LAG, Koffi KS, Ouattara L. Electrooxidation of the Paracetamol on Boron Doped Diamond Anode Modified by Gold Particles. International Research Journal of Pure & Applied Chemistry. 2021; 22(4): 23-35. DOI: 10.9734/IRJPAC/2021/v22i430401
18. Gnamba CQ-M, Appia FTA, Loba EMH, Sanogo I, Ouattara L. Electrochemical oxidation of amoxicillin in its pharmaceutical formulation at boron doped diamond (BDD) electrode. J. Electrochem. Sci. Eng. 2015; 5(2): 129-143; doi: 10.5599/jese.186
19. El-Desoky HS, Ghoneim EM, Ghoneim MM. Voltammetric behavior and assay of the antibiotic drug cefazolin sodium in bulk form and pharmaceutical formulation at a mercury. Journal of Pharmaceutical and Biomedical Analysis. 2005; 39 (5): 1051-1056. https://doi.org/10.1016/j.jpba.2005.05.020
20. Wudarska E, Chrzescijanska E, Kusmierek E. Electroreduction of Salicylic Acid, Acetylsalicylic Acid and Pharmaceutical Products Containing these Compounds. Portugaliae Electrochimica Acta. 2014; 32(4): 295-302. DOI: 10.4152/pea.201404295.

21. Wang D, Liu J, Wu Z, Zhang J, Su Y, Liu Z, Xu C. Electrooxidation of Methanol, Ethanol and 1-Propanol on Pd Electrode in Alkaline Medium. Int. J. Electrochem. Sci. 2009; 4: 1672 – 1678.
22.19. Belhadj–Tahar N, Savall A. Mechanistic Aspect of Phenol Electrochemical Degradation by oxidation on a Ta/PbO_2 Anode. J. electrochem. Soc. 1998; 145: 3427-3434. https://doi.org/10.1149/1.1838822
23. Samet Y, Elaoud SC, Ammar S, Abdelhedi R. Electrochemical degradation of 4-chloroguaiacol for waste water treatment using PbO_2 anodes. Journal of Hazardous Materials. 2006; 138: 614-619. https://doi.org/10.1016/j.jhazmat.2006.05.100
24. Murthy A, Manthiram A. Electrocatalytic oxidation of methanol to soluble products on polycrystalline platinum: Application of convolution potential sweep voltammetry in the estimation of kinetic parameters. Electrochimica Acta. 2011; 56(17): 6078-6083. https://doi.org/10.1016/j.electacta.2011.04.078
25. Appia FTA, Gnamba CQ-M, Kambiré O, Berté M, Sadia SP, Sanogo I, Ouattara L. Electrochemical Oxidation of Amoxicillin in Its Commercial Formulation on Thermally Prepared RuO_2/Ti. J. Electrochem. Sci. Technol. 2016 ; 7(1) : 82-89. DOI: http://dx.doi.org/10.5229/JECST.2016.7.1.82
26. Wudarska E, Chrzescijanska E, Kusmierek E, Rynkowski J. Voltammetric studies of acetylsalicylic acid electrooxidation at platinum electrode. Electrochimica Acta. 2013; 93: 189–194. http://dx.DOI: 10.1016/j.electacta.2013.01.107
27. Nagaraj PS, Shweta JM, Sharanappa TN. Electrochemical behavior of an antiviral drug acyclovir at fullerene-C60-modified glassy carbon electrode. Bioelectrochemistry. 2012; 88: 76-83. https://doi.org/10.1016/j.bioelechem.2012.06.004
28. Masek A, Chrzescijanska E, Zaborski M. Electrooxidation of morin hydrate at a Pt electrode studied by cyclic voltammetry. Food Chemistry. 2014; 148: 18–23. https://doi.org/10.1016/j.foodchem.2013.10.003
29. Masek A, Chrzescijanska E, Zaborski M. Estimation of the Antioxidative Properties of Amino Acids – an Electrochemical Approach. Int. J. Electrochem. Sci. 2014; 9: 7904 – 7915.
30. Aboul-Enein HY, Sibel AO. Electroanalytical Methods in Pharmaceutical Analysis and Their Validation. Chromatographia. 2012; 75: 811. DOI 10.1007/s10337-012-2268-7
31. Liu X, Luo L, Ding Y, Ye D. Poly-glutamic acid modified carbon nanotube-doped carbon paste electrode for sensitive detection of L-tryptophan. Bioelectrochemistry. 2011; 82(1): 38–45. https://doi.org/10.1016/j.bioelechem.2011.05.001
32. Fotouhi L, Fatollahzadeh M, Heravi MM. Electrochemical Behavior and Voltammetric Determination of Sulfaguanidine at a Glassy Carbon Electrode Modified with a Multi-Walled Carbon Nanotube. International Journal of Electrochemical Science. 2012; 7: 3919–3928.
33. Nambudumada SP, Jamballi GM. Polymethionine modified carbon nanotube sensor for sensitive and selective determination of L-tryptophan. J. Electrochem. Sci. Eng. 2020; 10(4): 305-315. http://dx.doi.org/10.5599/jese.774
34. Burcu D-T, Burcin B-P, Bengi U, Sibel AO. Multi-walled carbon nanotube modified glassy carbon electrode as a voltammetric nanosensor for the sensitive determination of anti-viral drug valganciclovir in pharmaceuticals. Sensors and Actuators B. 2013; 177: 841–847. http://dx.doi.org/10.1016/j.snb.2012.11.111
35. Koffi KM, Ouattara L. Electroanalytical Investigation on Paracetamol on Boron-Doped Diamond Electrode by Voltammetry. American Journal of Analytical Chemistry. 2019; 10: 562-578. https://doi.org/10.4236/ajac.2019.1011039